Bull. Soc. géol. Fr., 2010, t. 181, n° 1, pp. 19-26

Isostatic response and geomorphological evolution of the Nile valley during the Messinian salinity crisis

JULIEN GARGANI[1], CHRISTOPHE RIGOLLET[2,3] and SONIA SCARSELLI[4]

Key-words. – River, Erosion, Evaporites, Vertical movement, Climate

Abstract. – During the Messinian salinity crisis (5.96-5.33 Ma), the Mediterranean Sea was disconnected from the Atlantic Ocean. As a consequence, a dramatic sea-level fall occurred during part of the crisis and deep erosion has been observed on the Mediterranean margins as well as on the continent. Here, we demonstrate that the erosion and the large sea-level fall generated a significant uplift along the Nile River delta valley, due to isostatic rebound. Based on a quantitative analysis, our results suggest that the uplift of the Egyptian margin and of the Nile valley flanks may have triggered an enclosed environment during the Messinian salinity crisis (MSC). We estimated a mean rate of regressive erosion of -2.5 m/y along the River Nile during the MSC and of 1.25 and 0.4 m/y for the smaller rivers. The water discharge of the River Nile necessary to trigger this erosion rate was at least 5 to 25 times superior than the water discharge of the smaller one's.

Rebond isostatique et évolution géomorphologique de la vallée du Nil durant la crise Messinienne

Mots-clés. — Rivière, Erosion, Evaporites, Mouvements verticaux, Climat

Résumé. – Durant la crise de salinité messinienne (5,96-5,33 Ma), la mer Méditerranée fut déconnectée de l'océan Atlantique. En conséquence, un abaissement important du niveau de la mer Méditerranée s'est produit et une érosion d'une grande ampleur a eu lieu sur les marges et sur les continents. L'érosion Messinienne dans la vallée du Nil, ainsi que la baisse du niveau marin dans le bassin oriental, ont généré des mouvements verticaux importants dans la zone, à cause du rebond isostatique. Les déformations associées pourraient avoir généré des environnements confinés, comme des lacs. Ces mêmes déformations pourraient également avoir inversé la direction de drainage des rivières aux débits les plus faibles. Le taux moyen d'érosion régressive a été estimé à ~2,5 m/an le long du Nil Messinien et de 1,25 à 0,4 m/an pour les canyons plus petits sur la marge égyptienne. Le débit liquide nécessaire pour générer ces érosions est 5 à 25 fois supérieur pour le Nil que pour les autres canyons sur la marge égyptienne.

INTRODUCTION

Surface processes trigger mass movement on the surface of the Earth. One of the consequences of these mass movements is the loading or unloading of the lithosphere, as well as the morphological evolution of the Earth surface. Indeed, the loading/unloading of the lithosphere can generate vertical motions of the Earth surface. This phenomenon is called isostasy. Then, uplift and subsidence of the Earth surface produce erosion or sedimentation (mass movement) by a feedback process. These surface processes are of special interest to understand the Earth history.

One of the most spectacular event of mass movement occurred in the Mediterranean area around 6 million years ago. Deep erosion, giant evaporite bodies and dramatic sea water fall played a significant role during this period of time [Hsu *et al*., 1977; Ryan and Cita, 1978] called the Messinian salinity crisis (MSC). This event is an interesting example to study the consequences of surface processes on morphological evolutions of the Earth.

Isostatic rebound is expected to happen as a consequence of the large sea level fall, deep erosion and evaporite loading that occurred during the MSC [Gargani 2004a; Govers *et al*., 2008]. Recently, Scarselli *et al.* [2006 suggested that there is probably a genetic link between the major tectonic activity that occurred during the MSC and sea-level drawdown, on the basis of the river draining analysis in the Marche Apennines mountain range (Italy). The isostatic rebound has been quantified for the western Mediterranean basin [Norman and Chase, 1986; Gargani, 2004a and 2004b].

In the eastern basin, the sea level fall was different from that in the western basin due to the Sicily sill, which disconnected the eastern basin from the western basin. So, the consequences of the sea level fall in the Mediterranean area should be studied specifically for each sub-basin. Here, we

1. University of Paris-Sud, Lab. IDES, 91405 Orsay, France, julien.gargani@u-psud.fr
2. GDF, 361 Avenue du Président Wilson, 93211 Saint-Denis, France
3. now at BRGM, 3 av. Claude Guillemin, 45060 Orléans, France, c.rigollet@brgm.fr
4. ESSO Norge, 4064 Stavanger, Norway, sonia.scarselli@exxonmobil.com
Manuscrit déposé le 19 novembre 2008 ; accepté après corrections le 20 avril 2009.

study the amplitude of the isostatic rebound due to evaporite loading, sea water unloading and erosion, which affected the eastern Mediterranean basin and the Nile delta valley during the MSC, as well as the regressive erosion of the River Nile during this exceptional event. Then, the consequences of vertical movements on the geomorphological evolution of the Nile delta are discussed.

GEOLOGICAL BACKGROUND

In the last 30 years, evidence of deep erosion has been observed along the Mediterranean margins [Chumakov, 1973; Clauzon, 1973; Hsu *et al*., 1977; Ryan and Cita, 1978; Barber, 1981]. Valley incision occurred during the Messinian salinity crisis (MSC) after one [Bertoni and Cartwright, 2007], or eventually more [Gargani and Rigollet, 2007], large sea level falls of more than 1,200 m. Significant erosion of the central European Alps happened during the same period [Willett *et al*., 2006]. Contemporaneously, the periodical activation of coarse-grained deltaic systems of incised valleys in the Marche Appenines (Italy) is characteristic of catastrophic fluvial floods [Roveri and Manzi, 2006]. More generally, the major erosion, which affected the Mediterranean area is believed to be contemporaneous with an high precipitation rate [Griffin, 2002]. Nevertheless, precipitation was probably not distributed homogeneously in space [Gladstone *et al*., 2007] and time [Bertini, 2006; Rouchy and Caruso, 2006] during the MSC.

The amplitude and the number of the sea level falls depend on complex interactions between the global glacio-eustatic variations, climate and tectonic dynamics of the various thresholds, which separate the Mediterranean sub-basins [Blanc, 2000; Gargani and Rigollet, 2007]. These processes also contributed to the large accumulation of ~2,000 m of basinal evaporites in the Mediterranean Basin during the MSC [Hsu *et al*., 1977; Lofi *et al*., 2007; Gargani *et al*., 2008]. The duration of the sea-level main low-stand is probably less than 100 kyr, whereas the duration of the whole MSC is estimated to be circa 630 kyr [Krijgsman *et al*., 1999; 2007]. The end of the MSC could be due to the regressive erosion that affected the strait of Gibraltar [Blanc, 2002; Loget *et al*., 2005; Loget and Van Den Driessche, 2006].

The deeply incised River Nile (North East Africa, fig. 1) did not exist prior to the Messinian. Before the MSC, it is believed that the drainage of southern Egypt was dominated by a river (River Qena) that drained southwards east of the present River Nile [Issawi and McCauley, 1992; Goudie, 2005]. Geomorphological and sedimentary arguments, climate modelling and isotopic analysis suggest that a humid climate may have existed during the Late Miocene in North Africa [Griffin, 1999; 2002; Segueni, 2007; Gladstone *et al*., 2007]. The successive reorientation of the drainage pattern toward its present-day configuration could be due (i) to the capture of the River Qena by the headward erosion of the Eonile that was flowing more north [Goudie, 2005] during the MSC, (ii) to a dramatic change of the climatic conditions during this period [Griffin, 1999; 2002], or (iii) to a tectonic evolution of northeastern Africa.

The main deposits of the Nile valley are the Qawasim formation, the Rosetta anhydrite and the Abu Madi formation [Rizzini *et al*., 1978]. These sediments were deposited in the Nile delta during the MSC. The Qawasim formation overlies earlier mainly marine Miocene sediments [Griffin, 1999] and was deposited during the Messinian draw-down

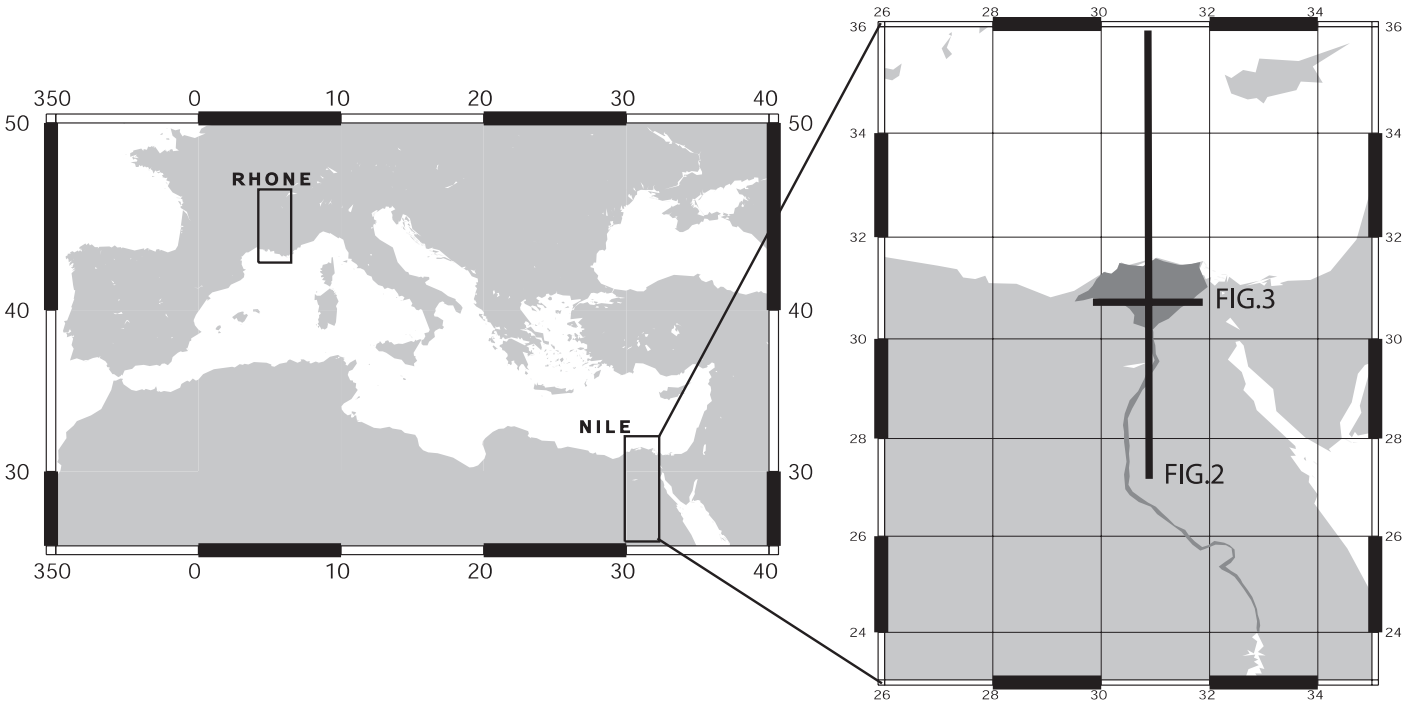

FIG. 1. – (A) Localisation map of the Nile and Rhône valleys. (B) Localisation of the sections used in figure 2 and 3.
FIG. 1. – (A) *Schéma de localisation des vallées du Nil et du Rhône.* (B) *Localisation sur la côte égyptienne de la vallée du Nil actuel et de l'emplacement des figures 2 et 3.*

of the eastern Mediterranean [Abdel *et al.*, 2000]. This sequence is composed of layers of sands, sandstones and conglomerates interbedded with occasional clay beds. The Abu Madi formation overlies the Rosetta anhydrites and is contemporaneous with an intra-Messinian unconformity [Abdel *et al.*, 2000]. Lagoonal deposits of Messinian age have been described on the shelf in the Nile delta area [Keheila, 1990. The Plio-Quaternary sediment infilling that loaded the Nile delta produced a low isostatic positive anomaly of around 300 m [Segev *et al.*, 2006].

METHOD

Using a 2D elastic model of the lithosphere [Weissel and Karner, 1989], we have calculated the vertical movement caused by the sea-water unloading and the sediment accumulation along a dip section perpendicular to the Egyptian Margin (fig. 2). The sea level fall simulated (1,500-2,500 m) is based on the estimates of Gargani and Rigollet [2007]. The thickness of the evaporites is believed to be of ~2,000 m [Hsu *et al.*, 1977; Loncke *et al.*, 2006]. The lithosphere is

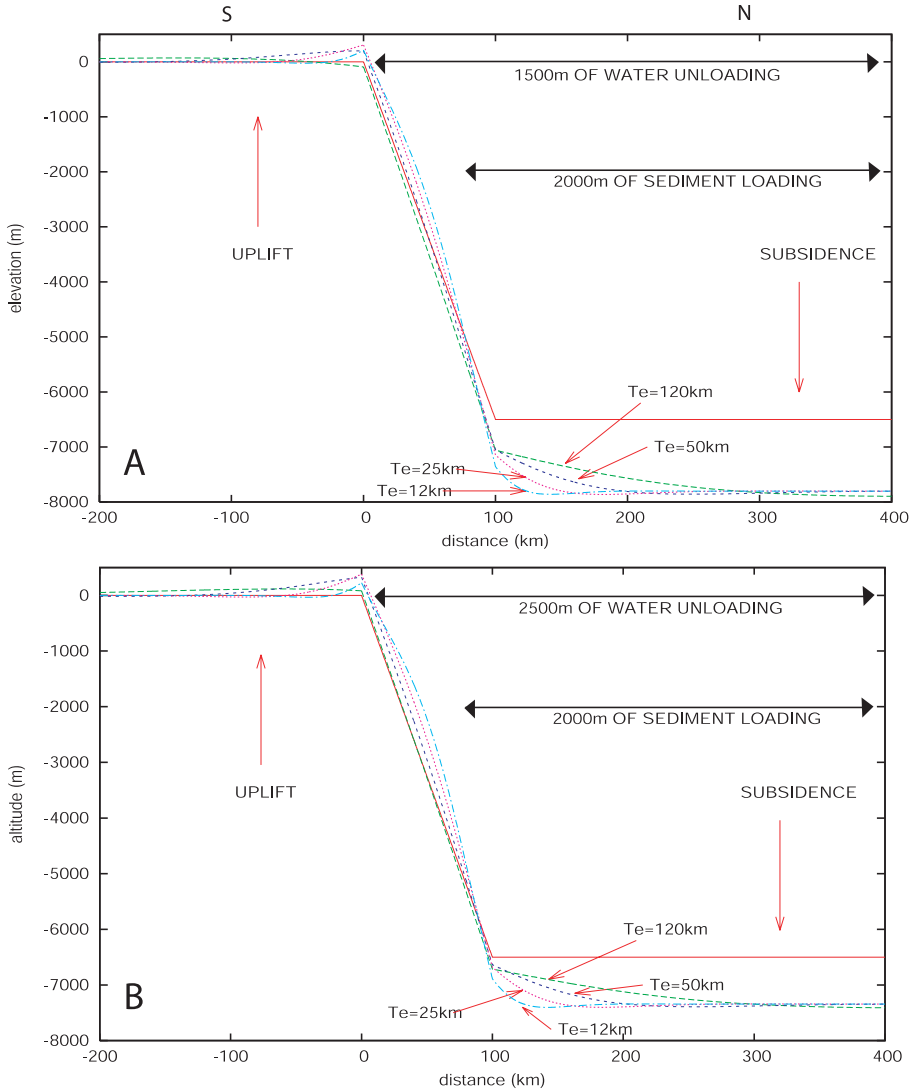

FIG. 2. – Isostatic rebound due to the sea level fall and the sediment accumulation during the Messinian salinity crisis in the eastern Mediterranean basin. The Messinian surface at the initial state (before isostatic deformation) is represented by the red line. The effect of the isostatic rebound is represented (A) for a sea level fall of 1,500 m in the whole eastern Mediterranean basin (unloading applied when x>0 km) and a loading of 2,000 m of evaporites in the centre of the basin (x>70 km), (B) for a sea level fall of 2,500 m in the whole eastern Mediterranean basin (unloading applied when x>0 km) and a loading of 2,000 m of evaporites in the centre of the basin (x>70 km). The subsidence of the centre of the basin is triggered by the sediment loading. The uplift and the smaller subsidence in case B in comparison to case A is due to the major sea water unloading. Various values of the elastic thickness T_e (in km) have been tested. ν=0.25, g=9.8 m·s^{-2}, ρ_{crust}=2,800 kg·m^{-3}, $\rho_{evaporite}$=2,170 kg·m^{-3}, ρ_{water}=1,000 kg·m^{-3}, ρ_{mantel}=3,300 kg·m^{-3}.

FIG. 2. – *Rebond isostasique causé par la chute du niveau marin et l'accumulation de sédiments durant la crise messinienne dans le bassin oriental de la Méditerranée en partant d'un état initial représenté par la ligne rouge* (A) *pour une chute du niveau marin de 1 500 m dans le bassin oriental et une accumulation de 2 000 m d'évaporites dans le centre du bassin (pour simuler le rebond isostasique, différentes valeurs de l'épaisseur élastique T_e (en km) ont été testées), (B) pour une chute du niveau marin de 2 500 m dans le bassin oriental et une accumulation de 2 000 m d'évaporites dans le centre du bassin. Pour effectuer les calculs, plusieurs valeurs pour l'épaisseur élastique T_e (en km) ont été testées.*
La subsidence du centre du bassin est générée par le poids des sédiments. Le soulèvement majeur de la partie la plus continentale de la marge et la subsidence plus faible du centre du bassin dans le cas B par rapport au cas A est provoqué par la baisse plus importante du niveau marin. ν=0.25, g=9.8 m·s^{-2}, ρ_{crust}=2 800 kg·m^{-3}, $\rho_{evaporite}$=2 170 kg·m^{-3}, ρ_{water}=1 000 kg·m^{-3}, ρ_{mantel}=3 300 kg·m^{-3}.

considered at the isostatic equilibrium before any loading (evaporites) or unloading (erosion, sea water fall) occurred. No horizontal forces are considered. There is no vertical movement at the boundary of the model. The model is taken sufficiently large to let the area of interest, around the margin, independent of the boundary condition. In the classical model of a thin infinite elastic plate, the mechanical behaviour is determined by the flexural rigidity D:

$$D = ET_e^3/[12(1-\nu^2)]$$

where E is the Young's modulus, T_e is the effective elastic thickness and ν is the Poisson's ratio. If E and ν are constants, the elastic thickness T_e is strictly proportional to the flexural rigidity D. In this case, the more the flexural rigidity D (and so T_e) is, the less the deformation is localized. Flexural rigidity values are often considered to be between 10^{21} and 10^{24} Nm [Norman and Chase, 1986; Weissel and Karner, 1989; Gargani, 2004a]. T_e is not necessarily proportional to the lithosphere or to the crust thickness. Considering that υ is equal to 0.25 and $E=10GPa$, the elastic thickness T_e will range between 12 and 120 km, respectively. In the model presented in figure 2, the effect of a loading of 2,000 m of evaporites in the central part of the eastern Mediterranean basin has been implemented. To simulate the sediment onlap on the margin, the loading of 2,000 m of evaporites is considered to occur from x=100 km offshore, where x is the distance from the Messinian coastline (fig. 2), and to decrease linearly until the margin (x=70 km offshore). The unloading of the water column above the margin has been considered to increase linearly from x=0 km until x=23 km (if the sea level fall is of 1,500 m, fig. 2A) or x=38 km (if the sea level fall is of 2,500 m, fig. 2B). Then, along the North-South profile, a constant unloading of the basin simulates the sea level fall of 1,500 m or 2,500 m. A simplified geometry of the present surface of the base of the MSC is assumed for the margin and the centre of the basin (fig. 2), as well as for the Nile delta valley (fig. 3) [Barber, 1981; Loncke, 2002]. The estimates of the deformation during the MSC could be affected by this simplified geometry. Indeed, the location of the area of evaporite loading and sea-water unloading play a role on the precise location of the area that uplifted during the Messinian. Nevertheless, this simplification does not influence significantly the results.

The geomorphological evolution of the Egyptian margin during the MSC is a consequence of deformation but also of erosion. The longitudinal profiles of rivers in the Nile delta before and at the end of the MSC have been used to constrain this evolution. The main Messinian valley of the Nile delta (Abu Madi valley, yellow crosses) with 4 smaller valleys observed in the Messinian Nile delta (fig. 4; red squares, blue crosses) have been superimposed on the same graph. We have used data published by Barber [1981] and industrial seismic lines to constrain the longitudinal profiles of rivers. The Messinian river profiles used are those observed at the present time and not those at the Messinian time. Nevertheless, the quantity of material eroded, that correspond to the material comprised between the initial profile (before erosion) and the final river profile

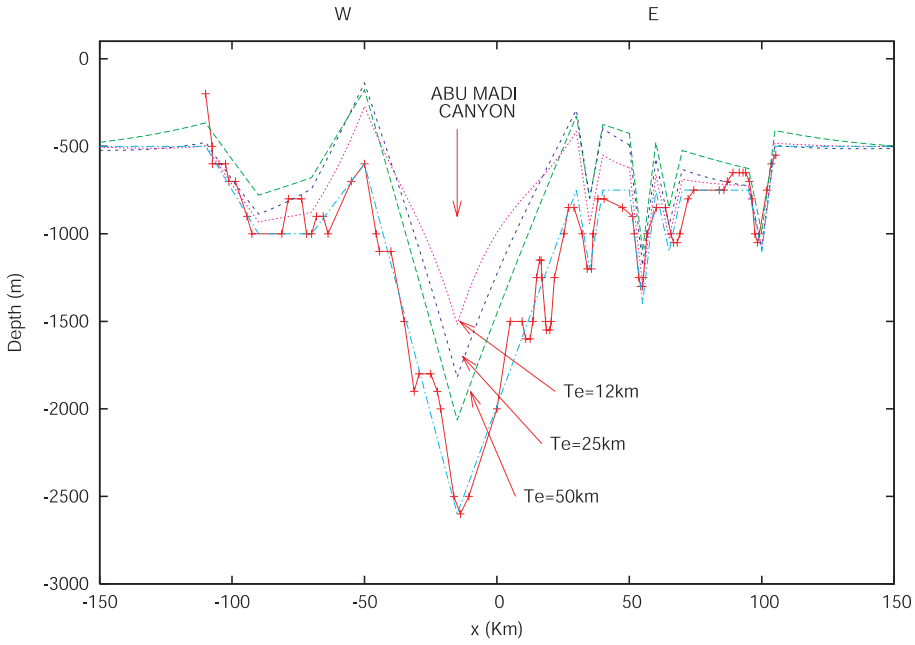

FIG. 3. – Isostatic rebound due to the large quantity of bedrock eroded during the MSC. The deep valley for which the various flexural rigidities have been tested is located 80 km north to Cairo parallely to the Hinge line (East-West direction, fig. 1B). The deeper valley is called "Abu Madi canyon". The Messinian valley morphology after erosion and before isostatic deformation is represented by the red line. For modelling simplicity, the blue line morphology is used to simulate the initial condition. Te= elastic thickness. ν=0.25, g=9.8 m·s^{-2}, ρ_{crust}=2,800 kg·m^{-3}, $\rho_{evaporite}$=2,170 kg·m^{-3}, ρ_{water}=1,000 kg·m^{-3}, ρ_{mantel}=3,300 kg·m^{-3}.

FIG. 3. – *Rebond isostatique causé par l'érosion importante du substrat durant la crise messinienne. La section de vallée pour laquelle les calculs ont été effectués se situe approximativement 80 km au nord du Caire, selon une direction Est-Ouest (voir fig. 1B). La vallée la plus profonde est connue sous le nom de canyon d'Abu Madi. La surface messinienne érodée avant déformation est représentée en rouge. Pour simplifier la modélisation, c'est la surface en bleu clair qui est utilisée lors de la simulation comme état initial avant déformation. Te= épaisseur élastique.* ν*=0.25, g=9.8 m·s*$^{-2}$, ρ_{crust}=2 800 kg·m^{-3}, $\rho_{evaporite}$=2 170 kg·m^{-3}, ρ_{water}=1 000 kg·m^{-3}, ρ_{mantel}=3 300 kg·m^{-3}.

(after erosion), will not change. As a consequence, the modelling of the quantity of material eroded is not affected by this simplification.

The regressive erosion has been modelled using the mass conservation equation:

$$\delta z(x,t)/\delta t = \delta Q_s(x,t)/\delta x$$

where z is the altitude, t is the time, Q_s is the sediment supply by unit length and x is the longitudinal distance. The sediment supply Q_s is considered proportional to the slope, the lithology k and the water discharge per unit length Q [Gargani *et al.,* 2006]:

$$Q_s(x,t) = k \cdot Q \cdot \delta z(x,t)/\delta x$$

To interpret the genesis of the longitudinal profile of the Messinian Nile valleys, a cumulated duration of 80 kyr for the main sea level low-stand in the western Mediterranean [Gargani and Rigollet, 2007] is modelled, in accordance with the small duration of the main drawdown phase [Krijgsman *et al.*, 1999]. The water discharge $Q=C \cdot x$ is considered to be linearly proportional to the distance x from the source and C a coefficient.

RESULTS AND DISCUSSION

Although a subsidence of the central part of the basin is expected, an uplift of the margin and of the continent occurred for all the flexural rigidity D tested (between 10^{21} Nm and 10^{24} Nm) and for both sea-level falls considered (1,500 m and 2,500 m). The amplitude of the uplift may reach a value of 400 m on the continent and around 800 m on the margin (fig. 2). In the basin, the subsidence ranges between 700 m and 1,400 m due to the accumulation of thick evaporites. The length of the area where uplift is expected depends on the flexural rigidity D. This length is comprised between 80 km and 200 km on the continent and on the margin depending of the amplitude of the sea level fall considered and on the flexural rigidity D assumed (fig. 2A and B).

An additional source of isostatic rebound is the large mass of rock eroded on the margin and on the continent. An incision of 2,000 m deep and 80 km wide occurred in the river Nile delta during the MSC [Barber, 1981]. The isostatic rebound triggered by the deep incision is estimated to range between 500 m and 1,000 m in the centre of the valley. On the flanks of the valley, 300-400 m of uplift are expected (fig. 3).

The evaporite loading into the basin partly counteract the effect of the sea water unloading and of the erosion on the continent and on the margin. The isostatic rebound probably increased the erosion by a feedback process. A previous estimation of the isostatic rebound in the Messinian Rhône valley area allowed interpretation of several field deformations data [Gargani, 2004b]. Due to the major erosion of the river Nile and to the greater sea level fall in the eastern Mediterranean basin than in the western one, the isostatic rebound is greater in the Nile delta valley (this study) than in the Rhône delta valley.

The influence of the sea level unloading on the deformation will be less significant considering a smaller sea level fall of ~1,200 m as suggested by Bertoni and Cartwright [2007], but still not negligible. A larger sea-level fall (>1,500 m) of the eastern Mediterranean Sea during the MSC is suggested by the vertical erosion of more than 1,500 m of the river Nile (fig. 4). Nevertheless, part of this

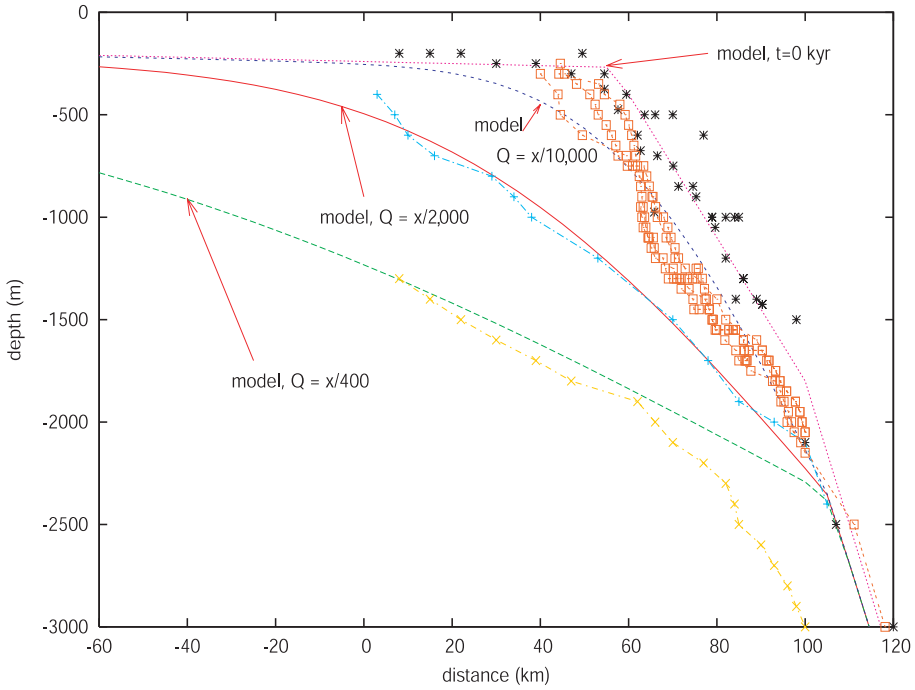

FIG. 4. – Longitudinal river profiles in the Nile delta before (black star) and at the end of the Messinian salinity crisis for small and intermediate valleys as well as the Abu Madi valley (red squares, blue crosses, yellow crosses respectively) compared with a numerical modelling. The regressive erosion is estimated to be of 2.5 m/yr for the Abu Madi valley. K=50. $Q_{Abu\ Madi}=5Q_{intermediate\ river}=25Q_{small\ river}$.

FIG. 4. – *Profils en long du Nil avant (croix noires) et après (carrées rouges pour les plus petites vallées, croix bleues pour les vallées de taille intermédiaire, croix jaunes pour la vallée d'Abu Madi) la crise Messinienne, comparés avec les résultats du modèle numérique. L'érosion régressive est estimée à 2,5 m/an pour la vallée d'Abu Madi. K=50.* $Q_{Abu\ Madi}=5Q_{rivière\ intermediaire}=25Q_{petite\ rivière}$.

incision could be due to the uplift (uplift=500-1,000 m) resulting from the isostasic rebound by a feedback process.

The combination of deep incision, regressive erosion, large sea level fall, evaporite loading and isostatic rebound produced a significant geomorphologic modification (fig. 5). The uplift of the margin and of the flanks of the valley should have triggered enclosed environment. A landward reversal of drainage in rivers may have happened due to the uplift of the shoreline. The reversal of drainage could allow a sufficient accumulation of water around the Nile delta to trigger the lacustrine environment observed by Keheila [1990]. Nevertheless, the Abu Madi valley was not affected by this phenomenon of reversal of drainage direction. Furthermore, the shoreline bulge increased the slope of the margin. These processes probably play a role in the incision of numerous canyon along the Egyptian margin.

This event probably triggered also a major reorganisation of the river drainage pattern. Indeed, the hydrological network may have also been affected by the possible capture of river Qena [Goudie, 2005] by a regressive erosion of the Abu Madi valley. Figure 4 shows the various longitudinal profiles in the Nile valley (Abu Madi and smaller valleys) during the MSC. These longitudinal profiles were affected by a regressive erosion as well as numerous areas along the Mediterranean margins. The simulation that better fits the longitudinal river profile evolution is obtained for a low stand of -2,100 m and regressive erosion rate of 2.5 m/year for the river Nile (fig. 4). For the smaller rivers, the regressive erosion rate was of 1.25 and 0.4 m/yr. The regressive erosion rate of the rivers of the Nile delta (Abu Madi valley as well as the other valleys) is of the same order of magnitude than the one of the river Rhône (~3 m/yr) during the MSC. The water discharge coefficient *C* of the river Nile that has been used to fit the data is 5 to 25 times greater than those of the smaller rivers.

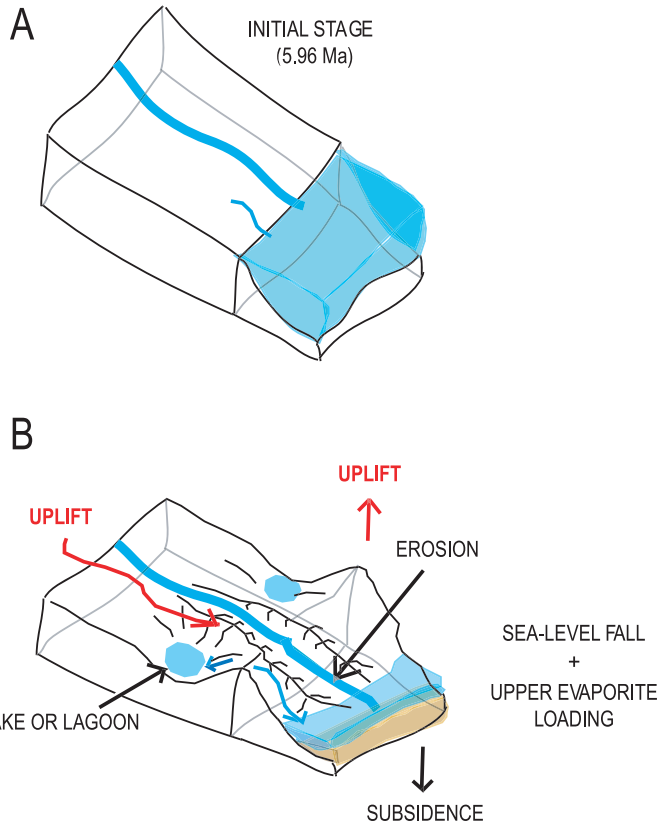

FIG. 4. – Geomorphological evolution of the river Nile during the Messinian salinity crisis. The sea-level fall triggered a deep incision. Contemporaneously, an isostatic rebound occurred that may have allowed to lakes or lagoons to form in the downstream part of the Nile river valley during the MSC.

FIG. 4. – *Schéma d'évolution géomorphologique du Nil durant la crise messinienne. La baisse du niveau marin a permis une érosion importante. Un rebond isostasique se produit alors. Ce rebond est susceptible de créer des lacs ou des lagons dans la partie aval du Nil.*

The Abu Madi valley was not deeply incised before the MSC as suggested by Issawi and McCauley [1992]. Nevertheless, the main valley of the Nile delta, i.e. the Abu Madi valley, was probably more developed than the other valleys at the beginning of the Mediterranean Sea fall. Indeed, the greater regressive erosion rate of the Abu Madi valley could be explained by (i) a greater water flux in comparison to the others valleys since the beginning of the MSC until the reflooding at the end of the MSC, and/or (ii) the capture of the river Qena that was flowing southward during the Miocene [Goudie, 2005].

Considering that all these valleys incised the same bedrock (*k* is constant), the difference between the different rates of regressive erosion is due to a difference in water discharge (fig. 4). The fact that the Abu Madi valley has a greater drainage area due to his longer length, but also that this drainage area was submitted to a mean precipitation rate > 3 mm/day in the southern part of Egypt, instead of 0.2-0.5 mm/day in the northern part during the MSC [Gladstone *et al*., 2007] for the smaller valleys could explain the difference in water discharge and in erosion rates. The modelling of erosion confirm that a significant water discharge should have occurred during the crisis. This fresh water discharge may explain a part of the evaporites accumulation in the deep basin [Gargani *et al*., 2008], as well as the detritic deposits of Messinian age in the Nile delta. The humid climate during the MSC allowed the genesis of numerous incised valleys.

The existence of wet conditions also before the crisis in North Africa [Brookes, 2001] could explain the existence of a hydrological network during the Miocene. As suggested before, the possible capture of the river Qena [Goudie, 2005] by a regressive erosion of the Abou Madi valley could also explain the development of a greater drainage area for the Abu Madi valley than for the other valleys. The capture of the river Qena that was flowing southward before, associated with a pre-existing Abu Madi valley [Issawi and McCauley, 1992] could explain the length of the river Nile. Our modelling study cannot allow discriminating if the capture of the river Qena occurred before or during the MSC.

CONCLUSION

Considering the deformations due to the sea-level fall and the sediment loading (fig. 2) as well as to the valley incision (fig. 3), the Nile valley is expected to have been significantly modified during the MSC. A shoreline bulge, triggered by the isostatic rebound due to the sea-water and erosion unloading, may have lead to a landward reversal of

drainage in rivers with low discharges as previously suggested by Norman and Chase [1986]. The Abu Madi valley was not affected by this phenomena and deeply incised the margin with significant erosion rates (fig. 4). This geomorphological evolution of the shoreline (fig. 5) may explain the enclosed environment (i.e. the existence of a lake or lagoon) that is believed to have existed during the MSC in the Nile delta [Keheila, 1990]. A capture as well a reorientation of the hydrological network that previously existed (river Qena) may be a consequence of the significant regressive erosion that happened during this period of time.

This evolution is a spectacular consequence of the complex interaction between erosion, isostatic deformations, sea-level fall and water discharge that occurred during the Messinian salinity crisis. One of the other possible consequences of these vertical movements and geomorphological modifications is the development of landslide on the shelf and on the margin during the MSC.

Acknowledgement. – The authors would like to thank the constructive comments from J. Lofi and an anonymous reviewer that improved the manuscript. GMT and Gnuplot have been used to draw figures 1-4.

References

ABDEL A., EL BARKOOKY A., GERRITS M., MEYER H., SCHWANDER M. & ZAKI H. (2000). – Tectonic evolution of the eastern Mediterranean Basin and its significance for hydrocarbon prospectivity in the ultradeep-water of the Nile delta. – The leading edge, 1086-1102.

BARBER P.M. (1981). – Messinian subaerial erosion of the Proto-Nile Delta. – *Mar. Geol.*, **44**, 253-272.

BERTINI A. (2006). – The northern Apennines palynological record as a contribute for the reconstruction of the Messinian palaeoenvironments. – *Sediment. Geol.,* **188-189**, 235-258.

BERTONI C. & CARTWRIGHT J.A. (2007). – Major erosion at the end of the Messinian salinity crisis: evidence from the Levant basin, eastern Mediterranean. – *Basin Res.,* **19**, 1-18.

BLANC P-L. (2000). – Of sills and straits: a quantitative assessment of the Messinian salinity crisis. – *Deep-Sea Res.,* **47**, 1429-1460.

BLANC P.L. (2002). – The opening of the Plio-Quaternary Gibraltar strait: assessing the size of a cataclysm. – *Geodin. Acta*, **15**, 303-317.

BROOKES I.A. (2001). – Possible Miocene catastrophic flooding in Egypt's western Desert. – *J. African Earth Sci.*, **32** , 325-333.

CHUMAKOV S. (1973). – Pliocene and Pleistocene deposits of the Nile valley in Nubia and Upper Egypt. *In*: W.B.F. RYAN *et al.,* Eds., *Int. Repts. DSDP*, U.S Govt. Printing Office, Washington, D.C., **13**, 1242-1243.

CLAUZON G. (1973). – The eustatic hypothesis and the pre-Pliocene cutting of the Rhône valley. *In*: W.B.F. RYAN *et al.,* Eds., *Int. Repts. DSDP*, U.S Govt. Printing Office, Washington, D.C., **13**, 1251-1256.

GARGANI J. (2004a). – Modelling of the erosion in the Rhône valley during the Messinian crisis (France). – *Quatern. Internat.,* **121**, 13-22.

GARGANI J. (2004b). – Eustatism, erosion and flexural isostasy: numerical modelling applied to the Messinian Rhône. – *C.R. Geoscience*, **336**, 901-907.

GARGANI J., STAB O., COJAN I. & BRULHET J. (2006). – Modelling the long-term fluvial erosion of the River Somme during the last million years. – *Terra Nova*, **18**, 118-129.

GARGANI J. & RIGOLLET C. (2007). – Mediterranean sea level variations during the Messinian salinity crisis. – *Geophys. Res. Lett.,* **34**, L10405, doi: 10.1029/2007GL029885.

GARGANI J., MORETTI I. & LETOUZEY J. (2008). – Evaporite accumulation during the Messinian salinity crisis: The Suez rift case. – *Geophys. Res. Lett.,* **35**, L02401, doi.10.1029/2007GL032494.

GLADSTONE R., FLECKER R., VALDES P., LUNT D. & MARWICK P. (2007). – The Mediterranean hydrologic budget from a Late Miocene global climate simulation. – *Palaeogeogr., Palaeoclimatol., Palaeoecol.,* **251**, 254-267.

GOUDIE A.S. (2005). – The drainage of Africa since the Cretaceous. – *Geomorphology*, **67**, 437-456.

GOVERS R., MEIJER P. & KRIJGSMAN W. (2008). – Regional isostatic response to Messinian salinity crisis events. – *Tectonophysics*, **463**, 109-129.

GRIFFIN D.L. (1999). – The late Miocene climate of northeastern Africa: unravelling the signals in the sedimentary succession. – *J. Geol. Soc.*, London, **156**, 817-826.

GRIFFIN D.L. (2002). – Aridity and humidity: two aspects of the late Miocene climate of North Africa and the Mediterranean. – *Palaeogeogr., Palaeoclimatol., Palaeoecol.,* **182**, 65-91.

HSU K.J., MONTADERT L., BERNOULLI D., CITA M.B., ERICKSON A., GARRISON R.E., KIDD R.B., MELIERES F., MULLER C. & WRIGTH R. (1977). – History of the Mediterranean salinity crisis. – *Nature*, **267**, 399-403.

ISSAWI B. & MCCAULEY J.F. (1992). – The Cenozoic rivers of Egypt: the Nile problem. *In*: B. ADAMS & R. FRIEDMAN, Eds., The followers of Horus. – Oxbow Press, Oxford, 1-18.

KEHEILA E. (1990). – Miocene facies models, paleoenvironments and sedimentary cycles in the Nile delta area, Egypt. – *J. African Earth Sci.,* **11**, issues 1-2, 221-230.

KRIJGSMAN W., HILGEN F.J., RAFFI I., SIERRO F.J. & WILSON D.S. (1999). – Chronology, causes and progression of the Messinian salinity crisis. – *Nature*, **400**, 652-655.

KRIJGSMAN W., HILGEN F.J. & MEIJER P.TH. (2007). – Chronological constraints and consequences for the Messinian salinity crisis. – *CIESM Workshop Monographs*, **33**, 39-44.

LOFI J., DEVERCHERE, J., GAULLIER V., GILLET H., GORINI C., GUENNOC P., LONCKE L., MAILLARD A., SAGE F., THINON I., CAPRON A. & OBONE ZUE OBAME E. (2007). – The Messinian salinity crisis in the offshore domain: an overview of our knowledge through seismic profile interpretation and multi-site approach. – *CIESM Workshop Monographs*, **33**, 83-90.

LOGET N., VAN DEN DRIESSCHE J. & DAVY P. (2005). – How did the Messinian salinity crisis end? – *Terra Nova*, **17**, 414-419.

LOGET N. & VAN DEN DRIESSCHE J. (2006). – On the origin of the strait of Gibraltar. – *Sediment. Geol.,* **188-189**, 341-356.

LONCKE L. (2002). – Le delta profond du Nil: structure et evolution depuis le Messinien. – PhD thesis, University of Paris 6, 230 pages.

LONCKE L., GAULLIER V., MASCLE J., VENDEVILLE B. & CAMERA L. (2006). – The Nile deep-sea fan: an example of interacting sedimentation, salt tectonics and inherited subsalt paleotopographic features. – *Mar. Petrol. Geol.,* **23**, 297-315.

NORMAN S.E. & CHASE C.G. (1986). – Uplift of the shores of the western Mediterranean due to Messinian desiccation and flexural isostasy. – *Nature*, **322**, 450-451.

RIZZINI A., VEZZANI F., COCOCCETTA V. & MILAD G. (1978). – Stratigraphy and sedimentation of Neogene-Quaternary section in the Nile delta area. – *Mar. Geol.,* **27**, 327-348.

ROUCHY J.-M. & CARUSO A. (2006). – The Messinian salinity crisis in the Mediterranean basin: a reassessment of the data and an integrated scenario. – *Sediment. Geol.*, **188-189**, 35-67.

ROVERI M. & MANZI V. (2006). – The Messinian salinity crisis: looking for a new paradigm? – *Palaeogeogr. Palaeoclimatol. Palaeoecol.*, **238**, 386-398.

RYAN W.B.F. & CITA M.B. (1978). – The nature and distribution of Messinian erosional surfaces indicators of a several kilometer deep Mediterranean in the Miocene. – *Mar. Geol.,* **27**, 193-230

SCARSELLI S., SIMPSON G., ALLEN P., MINELLI G. & GAUDENZI L. (2006). – Association between Messinian drainage network formation and major tectonic activity in the Marche Apennines (Italy). – *Terra Nova*, **19**, 74-81.

SEGEV A., RYBAKOV M., LYAKHOVSKY V., HOFSTETTER A., TIBOR G., GOLDSHMDT V. & BEN AVRAHAM Z. (2006). – The structure, isostasy and gravity field of the Levant continental margin and the southeast Mediterranean area. – *Tectonophysics*, **425**, 137-157.

SEGUENI F. (2007). – Etude des variations de la mousson nord Africaine et de l'hydrologie de l'Atlantique à la transition Mio-Pliocène: relations avec la crise de salinité messinienne en Méditerranée. – PhD thesis, Université Paris-Sud 11, France, 250 pages.

WEISSEL J.K. & KARNER G.D. (1989). – Flexural uplift of rift flanks due to mechanical unloading of the lithosphere during extension. – *J. Geophys. Res.,* **94**, 13,919-13,950.

WILLETT S.D., SCHLUNEGGER F. & PICOTTI V. (2006). – Messinian climate change and erosional destruction of the central European Alps. – *Geology*, **34**, 8, 613-616.